DOI: 10.1002/ ((please add manuscript number))
Article type: Full Paper

2,4,6-Triphenyl-1,3,5-triazine Based Covalent Organic Frameworks for Photoelectrochemical H_2 Evolution

Chunhui Dai, Ting He, Lixiang Zhong, Xingang Liu, Wenlong Zhen, Can Xue, Shuzhou Li, Donglin Jiang and Bin Liu**

Dr. C. Dai, Dr. X. Liu, Prof. B. Liu
Department of Chemical and Biomolecular Engineering
National University of Singapore
4 Engineering Drive 4, Singapore 117585, Singapore
Dr. T. He, Prof. D. Jiang
Department of Chemistry
Faculty of Science
National University of Singapore
3 Science Drive 3, Singapore 117543, Singapore
Dr. W. Zhen, Dr. L. Zhong, Prof. C. Xue, Prof. S. Li
School of Materials Science and Engineering
Nanyang Technological University
50 Nanyang Avenue, Singapore 639798, Singapore
Dr. C. Dai
Jiangxi Key Laboratory for Mass Spectrometry and Instrumentation, East China University of Technology, Nanchang 330013, P. R. China

Keywords: 2,4,6-triphenyl-1,3,5-triazine, covalent organic frameworks, photoelectrochemical H_2 evolution

Abstract: Photoelectrochemical water splitting over semiconductors offers a sustainable solar light conversion technique capable of alleviating worldwide energy crisis. Conjugated polymers have recently received increasing attention as a class of promising photoelectrode materials due to their advantages of earth-abundance, non-toxicity, light weight, and molecularly tunable functionalities, *etc*. However, the development of highly efficient organic photoelectrodes remains a big challenge. In this study, two covalent organic frameworks (COFs) incorporated 2,4,6-triphenyl-1,3,5-triazine have been demonstrated as excellent photocathodes for H_2 production. By introducing 2,4,6-triphenylbenene to properly create donor/acceptor pairs within COF, a significantly enhanced visible-light photocurrent of TAPB-TTB COF (110 $\mu A/cm^2$) compared to TTA-TTB COF (35 $\mu A/cm^2$) at 0 V *vs* reversible hydrogen electrode (RHE) was obtained without adding organic sacrificial agent and metal cocatalysts (> 420 nm).

The enhanced photocurrent density is attributed to the narrowed band gap and improved charge transfer by intramolecular donor-acceptor combination. This work highlights the great promising applications of crystalline donor-acceptor COFs as high-efficiency organic photoelectrode for water splitting.

Introduction

Over the past few decades, photoelectrochemical (PEC) water splitting for fuel production has attracted considerable research interest as an eco-friendly and low-cost approach for solar energy storage.[1-2] Since the first use of TiO_2 for this technique in 1972, inorganic compounds have been widely investigated as photoelectrode materials.[3-4] Recently, pure organic semiconductors have emerged as promising materials in PEC applications because of their highly tunable electronic properties by diverse synthetic modularity.[5] Polyacetylene photoelectrode was first reported for hydrogen generation in 1981, but its PEC activity was only 5.6 $\mu A/cm^2$ at -1.0 V versus Ag/AgCl electrode.[6] After that, more organic materials have been explored as photoelectrode for water splitting applications. This started with poly(thienylene),[7] polythiophene and derivatives,[8-9] followed by graphitic carbon nitrides (g-C_3N_4),[10-14] linear conjugated polymers.[15-19] However, while it is possible to tune optoelectronic properties like light absorption and energy levels by rational copolymerization strategies, organic polymers such as carbon nitrides and linear conjugated polymers are typically lack of crystallinity and show low surface areas. The lack of order could limit the transport of photoinduced charges to the electrode surface and lead to low photocurrent response under light irradiation. More generally, it is challenging to construct atomistic structure-property relationships for materials where the polymer architecture is poorly defined.

In this regard, covalent organic frameworks (COFs) is apt to overcome these drawbacks of aforementioned CPs by combining structural predictability, chemical versatility, as well as

high crystallinity and permanent porosity. The highly long-range ordered structure of COFs facilitates charge transfer and minimize charge trapping at defect sites. The structural porosity of COFs entails high BET surface areas, enabling both rapid charge diffusion to the material surface and easy accessibility of electrolytes throughout the COF sample deposited on the electrode. In particular, the recent years have seen a surge of interest in developing 2D COFs with outstanding optoelectronic properties, which provided new promise for photocatalysis/photoelectrocatalysis.[20,21] Unfortunately, although a large number of photoactive COFs with strong light harvesting and good charge separation capabilities have been reported, COFs have been rarely applied for PEC water splitting. In 2018, Bein and coworkers fabricated 2D COF film grown on conducting glass, which yielded a photocurrent response of 4.3 μA cm^{-2} at 0.3 V *vs* RHE.[22] Obviously, the potential of COF system for PEC water splitting has not been fully realized and the rational design of COFs with high PEC activity becomes an interesting research topic.

2,4,6-Triphenyl-1,3,5-triazine based COFs have recently been recognized as attractive porous materials with appealing semiconducting properties.[23-26] Notably, many of them have shown low interfacial resistance, enabling efficient charge transfer among the COFs. Inspired by this property, we studied two COFs based on 2,4,6-triphenyl-1,3,5-triazine for PEC H_2 evolution without additives under visible light. Introducing an electron donor (triphenylbenzene) was found to effectively decrease the optical gap and charge transfer of the resulting COFs, which yielded enhanced PEC performance, leading to a photocurrent up to ~110 μA/cm^2, greater than the ~35 μA/cm^2 from the TTA-TTB COF (structures shown in Scheme 1).

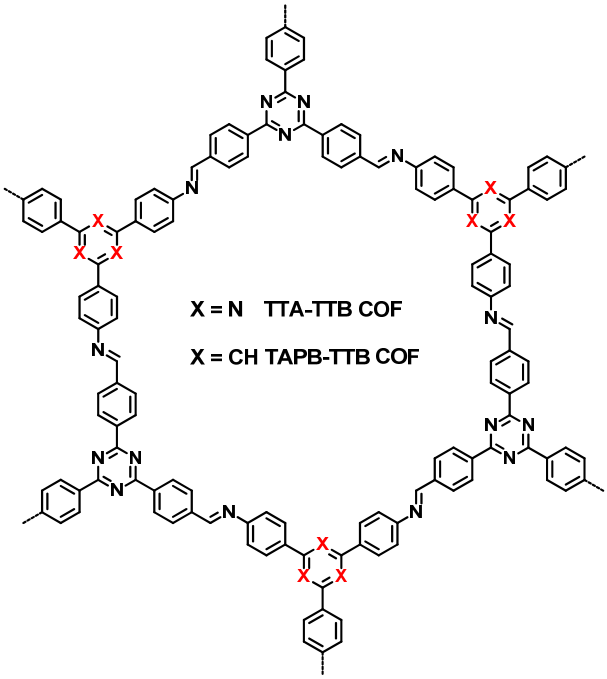

Scheme 1. Molecular structures of COFs for PEC H_2 evolution.

Results and Discussion

COF synthesis and characterization. TTA-TTB COF and TAPB-TTB COF were synthesized by polycondensation of 4,4',4"-(1,3,5-triazine-2,4,6-triyl)tribenzaldehyde (TTB) with 4,4',4"-(1,3,5-triazine-2,4,6-triyl)trianiline (TTA) and 1,3,5-tris(4-aminophenyl)benzene (TAPB), respectively. The reaction was conducted in a mixture of 1,4-dioxane and mesitylene in the presence of acetic acid at 120 ºC for 3 days (see the Supporting Information, **Scheme S1**). The FT-IR spectrum of COFs exhibited the characteristic peak of C=O (~1700 cm^{-1}) and the C–H (~CO-H vibrations (2819 and 2730 cm^{-1}) stretching in precursor aldehyde disappeared (**Figure S1**). In particular, the –C=N stretching peak of imine was observed at 1628 cm^{-1} for TTA-TTB COF and 1622 cm^{-1} for TAPB-TTB COF. Moreover, both COFs showed broad peaks at ~3400 cm^{-1}, which could be attributed to -N-H stretching in terminal NH_2 of COFs. In addition, scanning electron microscopy (SEM) images reveal that both COFs possess a granular morphology (**Figure S4**).

PXRD patterns of the two COFs reveal their excellent crystallinity nature (**Figure 1**a, b). In both cases, a strong diffraction peak assigned to the (100) facet was observed at a low angle, 2θ = 3.93° and 3.94° for TTA-TTB COF and TAPB-TTB COF, respectively, along with some other four peaks with relatively low diffraction intensities. These results are in accordance with previous reports.[27-29] The porosity of the two COFs is explored by the N_2 adsorption/desorption analysis, which displays a type-I isotherm indicative of mesoporous materials. The BET surface area of the TTA-TTB COF was evaluated to be 1592 m^2 g^{-1}, which is significantly higher than that of TAPB-TTB COF (932 m^2 g^{-1}, **Table 1**). As the PEC H_2 production reaction largely occurs at the interface between water and COF film, the larger BET surface area for TTA-TTB COF than that of TAPB-TTB COF could probably provide more active sites and attribute to the PEC efficiency. According to the nonlocal density function theory method (NL-DFT), the TTA-TTB COF and TAPB-TTB COF have mesopores of 2.2 and 2.19 nm, respectively, with pore volumes of 1.08 and 0.65 cm^3 g^{-1}. In addition, TGA curves of the two COFs showed that the degradation temperatures (T_d) of 5% weight loss of TTA-TTB COF and TAPB-TTB COF were 560 and 521 °C, respectively, which is attributed to the decomposition of the framework structure and the result indicates good thermal stability of the materials (**Figure S6**).

Optical and electrochemical properties. The rational design of D-A type conjugated polymers (CPs) by proper combination of electron donor (D) and acceptor (A) units has been widely used in polymer solar cells.[30-32] The intramolecular charge transfer (ICT) effect arising from the donor and acceptor interaction could facilitate π-electron delocalization, leading to a narrower band gap and desirable HOMO/LUMO energy levels. Owing to the electron push-pull interaction of the conjugated D-A system, the light absorption edge of TAPB-TTB COF is approximately 509 nm, which is red-shifted by about 44 nm over that of TTA-TTB COF (465 nm) (**Figure 1**c). The optical gaps were evaluated to be 2.43 eV for TTA-TTB COF and 2.67 eV for TAPB-TTB COF (Figure 1d). To determine the LUMO and HOMO energy levels of

COFs, electrochemical measurements in a deoxygenated nonaqueous electrolyte (anhydrous acetonitrile containning 0.1 M NBu_4PF_6) were carried out. The half-wave potential is 0.38 V versus Ag/Ag^+ with ferrocene (Fc) as the internal potential standard (**Figure S3**). From this, the LUMOs of TTA-TTB COF and TAPB-TTB COF were calculated to be -3.57 and -3.58 eV (**Table 1**), respectively. Using the optical band gap determined above, the HOMO positions are -6.24 eV for TTA-TTB COF and -6.01 eV for TAPB-TTB COF, respectively. Therefore, the driving force of both COFs is sufficient to drive water splitting under light irradiation.

Table 1. Summary of porosity data, optical gap, electrochemical properties and energy levels of the synthesized COFs.

COFs	S_{BET}[a)] ($m^2\ g^{-1}$)	Pore volume ($cm^3\ g^{-1}$)	Pore size (nm)	Band gap[b)] (eV)	E_{onset}[c)] (V)	LUMO[d)] (eV)	HOMO[e)] (eV)	Photocurrent ($\mu A/cm^2$)
TTA-TTB COF	1592	1.08	2.2	2.67	-0.85	-3.57	-6.24	35
TAPB-TTB COF	932	0.65	2.19	2.43	-0.84	-3.58	-6.01	110

[a]Specific surface area calculated from the N_2 adsorption isotherm. [b]Estimated from DRS absorption onset ($E_g = 1240/\lambda_{onset}$). [c]Versus Ag/Ag^+, scan rate is 50 mV s^{-1}, determined from the onset potentials of the reduction waves. [d]LUMO = $-(E_{red,onset} - E_{1/2,Fc,Fc+} + 4.8) = -(E_{red,onset} + 4.44)$ eV; [e]Estimated from $E_{HOMO} = E_{LUMO} - E_{g,opt}$.

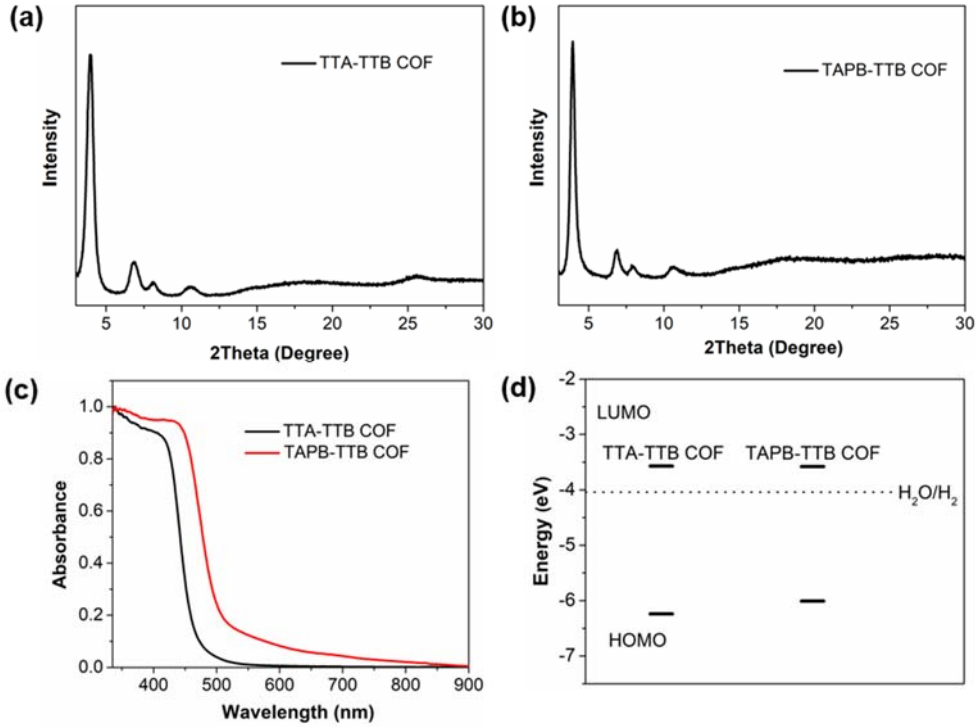

Figure 1. Powder XRD patterns (a,b), UV-vis diffuse reflectance spectra (c) and LUMO/HOMO positions (d) of TTA-TTB COF and TAPB-TTB COF.

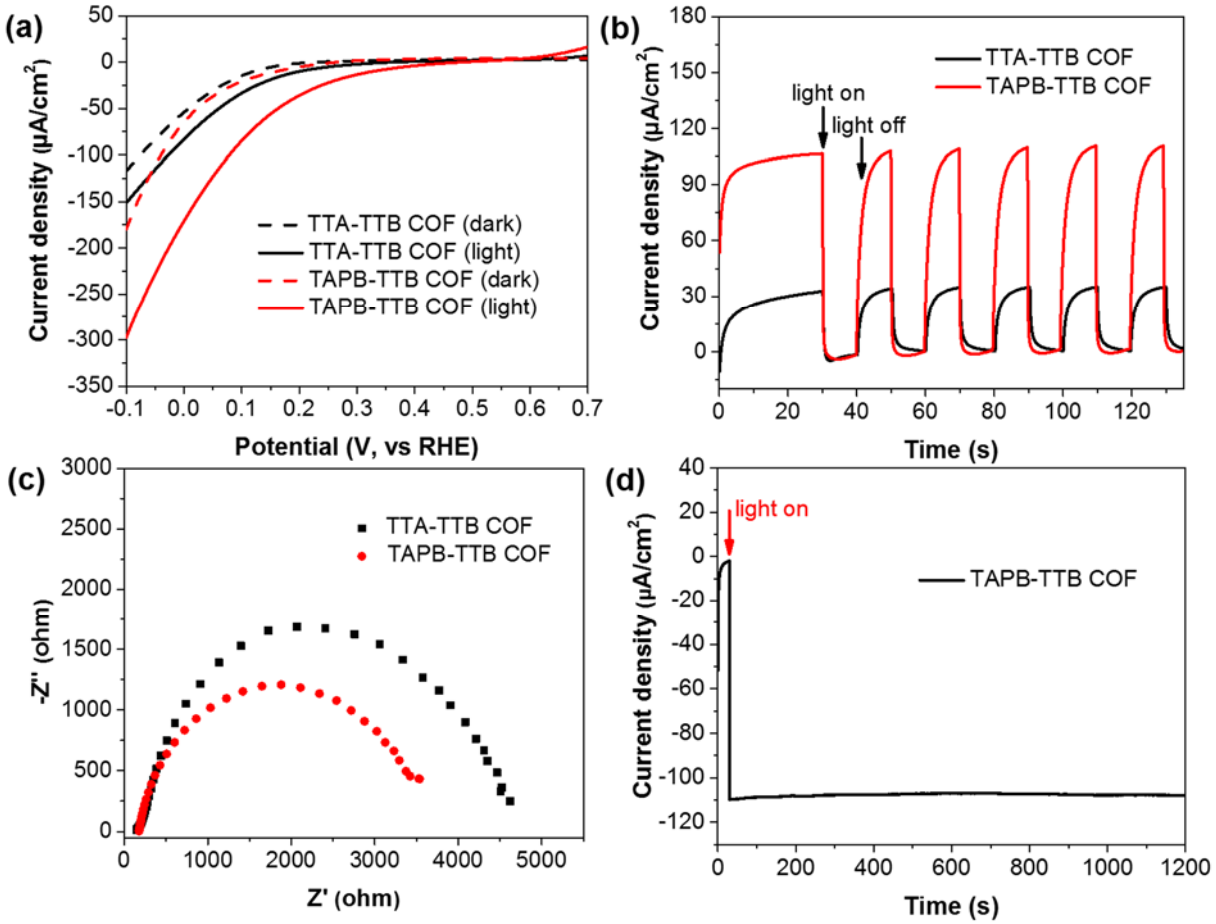

Figure 2 a) Linear sweep voltammetry (LSV) curves of TTA-TTB COF (black curve) and TAPB-TTB COF photoelectrodes (red curve), respectively, in 0.2 M Na_2SO_4 aqueous solution (pH 7) with and without visible light (> 420 nm); b) Photocurrent of COFs at 0 V vs. RHE upon on/off visible light irradiation; c) Electrochemical impedance spectroscopy (EIS) of COFs at 0 V vs. RHE; d) The current-time (i-t) curves for TAPB-TTB COF photoanode under visible light irradiation (> 420 nm).

Photoelectrochemical activities. The photoelectrochemical water reduction for the COF photoelectrodes were examined by current density-sweeping voltage (*J*-*V*) measurements in 0.5 M Na_2SO_4 (pH 7) under visible light. As displayed in **Figure 2**a, compared to TTA-TTB COF, TAPB-TTB COF presented a much larger photocurrent density with a cathodic shift of 35 mV in the onset potential for water reduction. Figure 2b revealed that TAPB-TTB COF electrode exhibited a current density of 110 μA cm^{-2} with a solar-to-hydrogen (STH) conversion

efficiency of 0.068% at 0 V versus the RHE, over 3 times higher than that of TTA-TTB COF. Notably, this PEC activity is excellent compared to previously reported organic photoanodes like poly(phenylene cyanovinylenes), g-C_3N_4, and fluorene dibenzothiophene-S,S-dioxide-based polymers, *etc* (**Table S1**). Compared to those amorphous organic polymer materials, the densely aligned π-arrays of COFs could act as pre-organized pathways to facilitate photoexcited charge transport for achieving good performance. The enhanced PEC activities of TAPB-TTB COF could be attributed to the D-A structure which enables broader visible-light absorption and more effective charge transfer as evidenced by the electrochemical impedance spectroscopy (EIS) measurements, which clearly exhibits a reduction in diameter of the semicircle TAPB-TTB COF in the Nyquist plot (Figure 2c). A durability test revealed that TAPB-TTB COF can maintain the photocurrent for ~1200 s (Figure 2d). In addition, no significant changes in the XRD or TGA were observed for both COFs after the PEC measurements, indicating that water-splitting does not cause any crystallinity variation or structural deformation of the COFs (Figure **S7**).

Theoretical calculations. DFT calculations were conducted to study the electronic properties of the two COFs, and to understand the significantly improved photoelectrochemical water splitting ability of TAPB-TTB COF. The optimized structures of the two COFs are shown in **Figure S8**, which adopt two dimensional hexagonal structures and the optimized structural parameters are similar: 25.92 and 25.71 Å for TAPB-TTB COF and TTA-TTB COF, respectively. The predicted HOMOs and LUMOs for TAPB-TTB COF and TTA-TTB COF are depicted in **Figure S9**. The HOMO potentials of both TAPB-TTB COF (1.68 V) and TTA-TTB COF (2.09 V) are much more positive than the one required for water oxidation to O_2 (0.82 V, pH = 7), and the LUMO potentials of both TAPB-TTB COF (-1.07 V) and TTA-TTB COF (-0.93 V) are similar and more negative than the potential of H^+/ H_2 (-0.41 V, pH = 7). These results confirm the sufficient driving force of the two COFs for water splitting.

The calculated band gaps for TTA-TTB COF and TAPB-TTB COF are 3.02 and 2.75 eV, respectively, which are in good agreement with the optical gap obtained in our experiments (2.67 eV for TTA-TTB COF and 2.43 eV for TAPB-TTB COF as shown in Table 1). As for electron-hole separation, TAPB-TTB COF is expected to be more effective because of stronger donor-acceptor interaction than TTA-TTB COF. **Figure 3**a and d show the atomic structure of TTA-TTB COF and TAPB-TTB COF, and the corresponding spatial distributions of excited electrons are presented in Figure 3b and e. For TAPB-TTB COF, the excited electrons are mainly located on the TTB moiety and the holes are mainly located on the TAPB moiety. While for TTA-TTB COF, the distributions of excited electrons and holes are much more uniform. The distinct distributions of excited electrons and holes in TAPB-TTB COF result in more effective electron-hole separation and dissociation as illustrated in Figure 3g. Therefore, the much better photoelectrochemical performance of TAPB-TTB COF comes from its smaller band gap and improved excitons dissociation because of stronger donor-acceptor interaction.

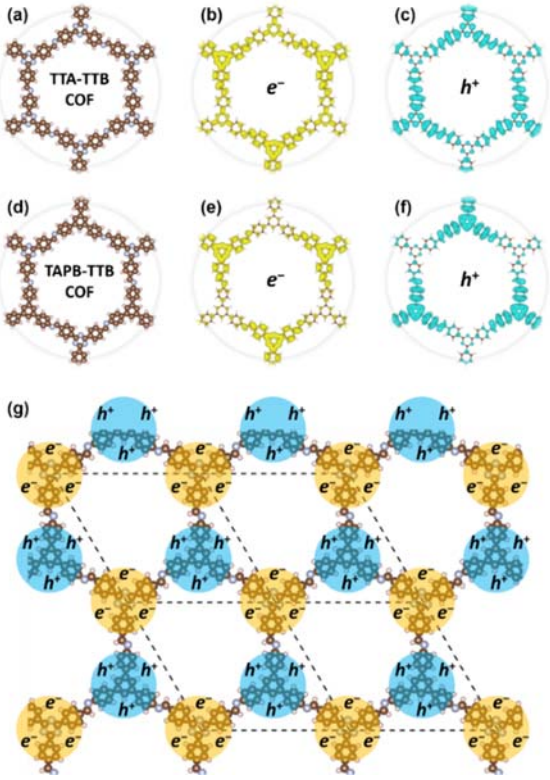

Figure 3 Optimized atomic structure by DFT calculations (a,d), spatial distributions of excited electrons (b,e) and holes (c,f) of TTA-TTB COF and TAPB-TTB COF. Schematic illustration of the effective separation between excited e^- and h^+ in TAPB-TTB COF (g).

Conclusions

In summary, we show that two 2,4,6-triphenyl-1,3,5-triazine based COFs are highly efficient photoelectrodes for water reduction under visible light. The construction of intramolecular donor-acceptor system is demonstrated as a practical strategy to significantly enhance the photocurrent response of 110 μA/cm^2 in neutral water without adding any sacrificial agents. The superior photocatalytic activity is attributed to the promoted charge transfer and extended light absorption, which was further analyzed using first principle calculations. This work demonstrates how comonomers in 2D COFs can be tuned to achieve synergetic interactions for PEC water splitting, thereby providing the basis for designing new organic photoelectrode.

Supporting Information

Supporting Information is available from the Wiley Online Library or from the author.

Author Information

Corresponding Author

*E-mail: cheliub@nus.edu.sg.

*E-mail: chmjd@nus.edu.sg.

Notes

The authors declare no competing financial interest.

Acknowledgements

C.H. D. and T. H. contributed equally to the work. Financial work was provided by the Singapore National Research Foundation (grant no. R279-000-444-281), the National

University of Singapore (grant no. R279-000-482-133), Research Foundation for Advanced Talents of East China University of Technology (No. DHBK201927), National Science Foundation for Young Scientists of China (grant no. 21905122), National Science Foundation of Jiangxi province of China (No. 20202BAB203007). D. J. acknowledges supports by MOE tier 1 grant (R-143-000-A71-114) and NUS start-up grant (R-143-000-A28-133). C. X. thanks the support from the Ministry of Education, Singapore, under AcRF-Tier2 (MOE2018-T2-1-017) and AcRF-Tier1 (MOE2019-T1-002-012, RG102/19).

References

[1] T. Hisatomi, J. Kubota, K. Domen, *Chem. Soc. Rev.* **2014**, 43, 7520.

[2] E. L. Miller, *Energy Environ. Sci.* **2015**, *8*, 2809.

[3] C. Jiang, S. J. A. Moniz, A. Wang, T. Zhang, J. Tang, *Chem. Soc. Rev.* **2017**, *46*, 4645.

[4] L. Yao, A. Rahmanudin, N. Guijarro, K. Sivula, *Adv. Energy Mater.* **2018**, *8*, 1802585.

[5] S. Otep, T. Michinobu, Q. Zhang, *Sol. RRL* **2019**, *4*, 1900395.

[6] H. Shirakawa, S. Ikeda, M. Aizawa, J. Yoshitake, S. Suzuki, *Synth. Met.* **1981**, *4*, 43.

[7] T. Kenmochi, E. Tsuchida, M. Kaneko, A. Yamada, *Electrochim. Acta* **1985**, *30*, 1405.

[8] E. M. Girotto, W. A. Gazotti, M.-A. De Paoli, *J. Phys. Chem. B* **2000**, *104*, 6124.

[9] U. Mengesha, T. Yohannes, *Sol. Energy Mater. Sol. Cells* **2006**, *90*, 3508.

[10] L. Ye, S. Chen, *Appl. Surf. Sci.* **2016**, *389*, 1076.

[11] X. Lu, Z. Liu, J. Li, J. Zhang, Z. Guo, *Appl. Catal., B* **2017**, *209*, 657.

[12] X. Lv, M. Cao, W. Shi, M. Wang, Y. Shen, *Carbon* **2017**, *117*, 343.

[13] Q. Gu, X. Gong, Q. Jia, J. Liu, Z. Gao, X. Wang, J. Long, Can Xue, *J. Mater. Chem. A* **2017**, *5*, 19062.

[14] Q. Ruan, W. Luo, J. Xie, Y. Wang, X. Liu, Z. Bai, C. J. Carmalt, J. Tang, *Angew. Chem. Int. Ed.* **2017**, *56*, 8221.

[15] P. Bornoz, M. S. Prévot, X. Yu, N. Guijarro, K. Sivula, *J. Am. Chem. Soc.* **2015**, *137*, 15338.

[16] M. Mansha, I. Khan, N. Ullah, A. Qurashi, M. Sohail, *Dyes Pigm.* **2017**, *143*, 95.

[17] M. Mansha, I. Khan, N. Ullah, A. Qurashi, *Int. J. Hydrogen Energy* **2017**, *42*, 10952.

[18] C. Dai, X. Gong, X. Zhu, C. Xue, B. Liu, *Mater. Chem. Front.* **2018**, *2*, 2021.

[19] H. Sun, I. H. Öner, T. Wang, T. Zhang, O. Selyshchev, C. Neumann, Y. Fu, Z. Liao, S. Xu, Y. Hou, A. Turchanin, D. R. T. Zahn, E. Zschech, I. M. Weidinger, J. Zhang, X. Feng, *Angew. Chem. Int. Ed.* **2019**, *58*, 10368.

[20] J. L. Segura, M. J. Mancheñoa, F. Zamora, *Chem. Soc. Rev.* **2016**, *45*, 5635.

[21] F. Beuerle, B. Gole, *Angew. Chem. Int. Ed.* **2018**, *57*, 4850.

[22] T. Sick, A. G. Hufnagel, J. Kampmann, I. Kondofersky, M. Calik, J. M. Rotter, A. Evans, M. Döblinger, S. Herbert, K. Peters, D. Böhm, P. Knochel, D. D. Medina, D. Fattakhova-Rohlfing, T. Bein, *J. Am. Chem. Soc.* **2018**, *140*, 2085.

[23] W. Huang, J. Byun, I. Rörich, C. Ramanan, P. W. M. Blom, H. Lu, D. Wang, L. Caire da Silva, R. Li, L. Wang, K. Landfester, K. A. I. Zhang, *Angew. Chem. Int. Ed.* **2018**, *57*, 8316.

[24] S.-Y. Yu, J. Mahmood, H.-J. Noh, J.-M. Seo, S.-M. Jung, S.-H. Shin, Y.-K. Im, I.-Y. Jeon, J.-B. Baek, *Angew. Chem. Int. Ed.* **2018**, *57*, 8438.

[25] M. Liu, Q. Huang, S. Wang, Z. Li, B. Li, S. Jin, B. Tan, *Angew. Chem. Int. Ed.* **2018**, *57*, 11968.

[26] X. Chen, Q. Dang, R. Sa, L. Li, L. Li, J. Bi, Z. Zhang, J. Long, Y. Yu, Z. Zou, *Chem. Sci.* **2020**, *11*, 6915.

[27] V. S. Vyas, M. Vishwakarma, I. Moudrakovski, F. Haase, G. Savasci, C. Ochsenfeld, J. P. Spatz, B. V. Lotsch, *Adv. Mater.* **2016**, *28*, 8749.

[28] F. Haase, K. Gottschling, L. Stegbauer, L. S. Germann, R. Gutzler, V. Duppel, V. S. Vyas, K. Kern, R. E. Dinnebier, B. V. Lotsch, *Mater. Chem. Front.* **2017**, *1*, 1354.

[29] P. Wang, Q. Xu, Z. Li, W. Jiang, Q. Jiang, D. Jiang, *Adv. Mater.* **2018**, *30*, 1801991.

[30] Y. Li, *Acc. Chem. Res.* **2012**, *45*, 723.

[31] H. Yao, L. Ye, H. Zhang, S. Li, S. Zhang, J. Hou, *Chem. Rev.* **2016**, **116**, 7397.

[32] C. Liu, K. Wang, X. Gong, A. J. Heeger. *Chem. Soc. Rev.* **2016**, *45*, 4825.

Keyword

2,4,6-triphenyl-1,3,5-triazine, covalent organic frameworks, photoelectrochemical, H_2 evolution

Chunhui Dai, Ting He, Lixiang Zhong, Xingang Liu, Wenlong Zhen, Can Xue, Shuzhou Li, Donglin Jiang,* and Bin Liu*

Title: 2,4,6-Triphenyl-1,3,5-triazine Based Covalent Organic Frameworks for Photoelectrochemical (PEC) H_2 Evolution

ToC figure